



MECHANICAL ENGINEERING PROJECT II

**ÇUKUROVA UNIVERSITY
DEPARTMENT OF MECHANICAL ENGINEERING**

BURAK YÖRÜKÇÜ

**PROJECT TITLE: Building Vortex Shedding and Wind Load
Analysis**

PROJECT SUPERVISOR: Doç.Dr. GÖKTÜRK MEMDUH ÖZKAN

SUBMISSION DATE:28.06.2024

Spring Term
2023-2024

CONTENTS

LIST OF FIGURES	1
INTRODUCTION	3
WHAT IS THE VORTEX SHEDDING?	4
VORTEX-STRUCTURE INTERACTION.....	5
VORTICITY GENERATION; VORTEX STREET	6
VORTEX SHEDDING HAZARDS.....	7
WIND LOAD ANALYSIS.....	8
INTRODUCTION PING AN FINANCE CENTER.....	9
DETAILS AND DETERMINING SPECIFICATIONS OF PROPERTIES	10
CALCULATIONS OF IMPORTANT PARAMETERS OF THE ANALYSIS	12
STROUHAL NUMBER	14
TIME STEP SIZE.....	15
ANALYSIS OF PING AN FINANCE CENTER IN ANSYS FLUENT	16
DISCUSSING THE RESULT OF ANALYSIS	22
OTHER ANALYSES RESULTS.....	27
FFT GRAPH FOR DIFFERENT ANALYSES	28
VELOCITY CONTOURS OF ANALYSES	29
RESULT OF ANALYSIS.....	30
REFERENCES	31

LIST OF FIGURES

Figure 1.0 Force Directions and Periodic Vortex Shedding Applied on Tall Building.	3
Figure 1.1 Vortex Shedding simulated by CFD Software.....	4
Figure 1.2 Vortex Shedding.	4
Figure 1.3 Vortex Interaction.....	5
Figure 1.4 Vortex-Structure Interaction.	6
Figure 1.5 Von Karman Vortex Shedding.	6
Figure 1.6 Tacoma Narrow Bridge.	7
Figure 1.7 Lateral Load on Tall Buildings.....	7
Figure 1.8 Oscillations on power lines.	7
Figure 1.9 Wind Load Over A Building.	8
Figure 2.0 Details of Building.....	9
Figure 2.1 Real Picture of the Building.....	9
Figure 2.2 Physical Properties of Air.	10
Figure 2.3 Average Temperature in Shenzhen.	11
Figure 2.4 Average Wind Speed in Shenzhen.....	11
Figure 2.6 Reynolds Number.	12
Figure 2.6 Critical Number for Reynolds in External Flows.	13
Figure 2.7 Strouhal Number.	14
Figure 2.8 Strouhal Number for Different Geometries.....	14
Figure 2.9 Time in Transient Simulation.....	15
Figure 3.0 Geometry of Structure.	16
Figure 3.1 Closed View of Geometry.	16
Figure 3.3 Meshed Structure.	17
Figure 3.4 Meshed Structure but Closer.....	17
Figure 3.5 Closest Picture of Meshed Structure.	18
Figure 3.6 Mesh Quality for Orthogonal.	18
Figure 3.7 Mesh Quality for Skewness.....	18
Figure 3.8 Number of Mesh.....	19
Figure 3.9 Skewness and Orthogonal Mesh Metric Spectrums.....	19
Figure 4.0 Scaled Residuals.	22
Figure 4.1 Drag Coefficient Graph.	23
Figure 4.2 Cd Values For Different Shapes.	24
Figure 4.3 Lift Coefficient Graph.....	24

Figure 4.4 FFT Graph.	25
Figure 4.5 Velocity Contour.	26
Figure 4.6 FFT Graph of 20m/s.	28
Figure 4.7 FFT Graph of 25m/s.	28
Figure 4.8. Velocity Countour of 20m/s.	Error! Bookmark not defined.
Figure 4.9 Velocity Contour of 25m/s.	29
Figure 4.11 Ping An Finance Center.	30

INTRODUCTION

Vortex shedding is a phenomena that can cause considerable vibrations in high-rise buildings. It occurs when wind flow generates alternating vortices. If these vibrations coincide with the inheret of the building, structural failure or damage may result. In the design stage, it is critical to comprehend and reduce vortex shedding effects in order to guarantee the stability and safety of tall structures.

This projects aims to investigate vortex shedding and its effects on high-rise buildings through ANSYS Fluent. This projects also aims look into wind load analysis in high-rise buildings. This projects analyze the formation and behavior of vortices around high-rise building as well as collects data with these datas the wind loads generated by vortex shedding and develop design recommendations to reduce these effects on high-rise buildings.

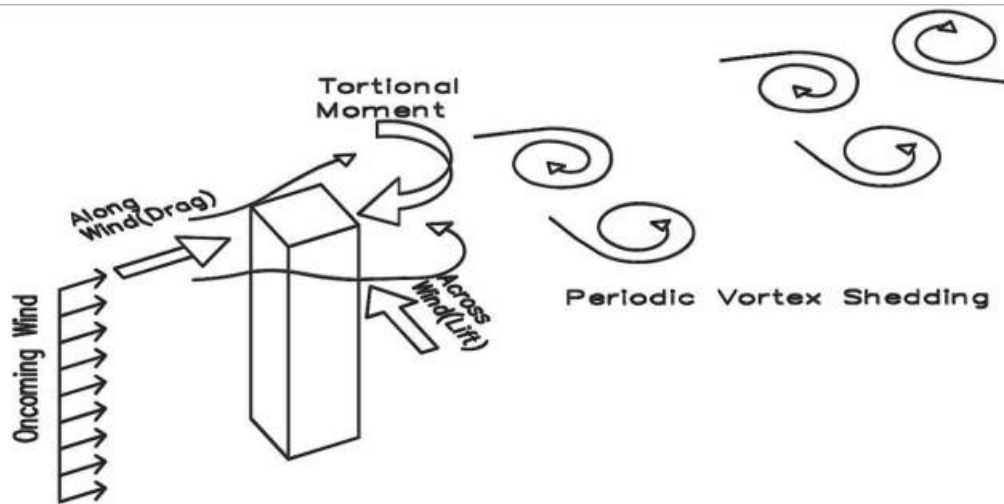


Figure 1.0 Force Directions and Periodic Vortex Shedding Applied on Tall Building.

WHAT IS THE VORTEX SHEDDING?

Vortex shedding is a phenomenon, when the wind blows across a structural member, vortices are shed alternately from one side to the other, and where alternating low-pressure zones are generated on the downwind side of the structure giving rise to a fluctuating force acting at right angles to the wind direction.

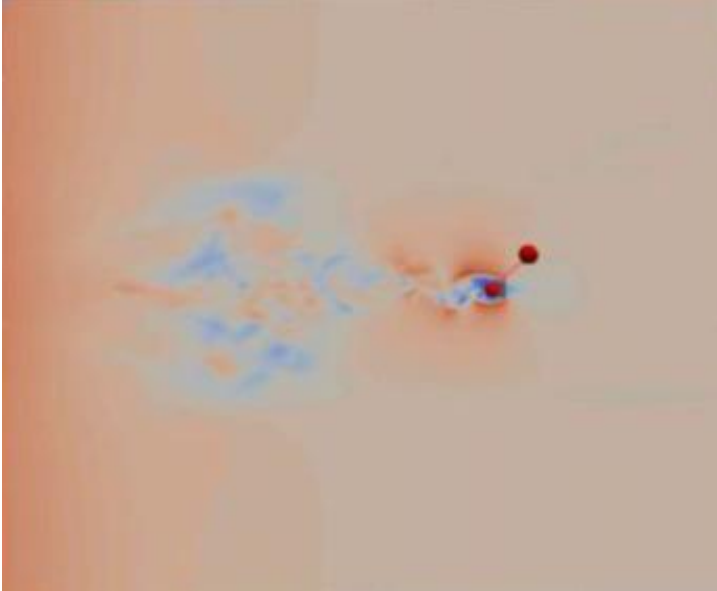


Figure 1.1 Vortex Shedding simulated by CFD Software.

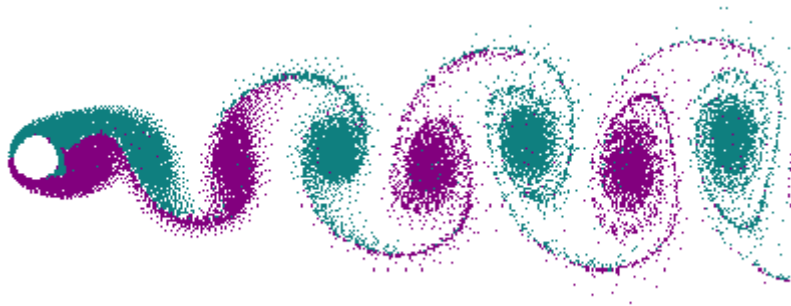


Figure 1.2 Vortex Shedding.

VORTEX-STRUCTURE INTERACTION

Vorticity is generated in the boundary layers of structures in fluid flows. The boundary layer vorticity convects aft and coalesces into discrete swirling vortices in the near wake. These vortices generate oscillations of the near wake. Feedback from the near wake oscillations to the separation points leads to the periodic shedding of vortices with alternate-sign circulation that form the famous von Karman vortex-street. Structural vibration and sound can synchronize with the periodic vortex shedding. Vortex shedding can induce damaging large-amplitude vibrations of flexible structures in fluid flows and produce intense acoustic pressures in ducts.

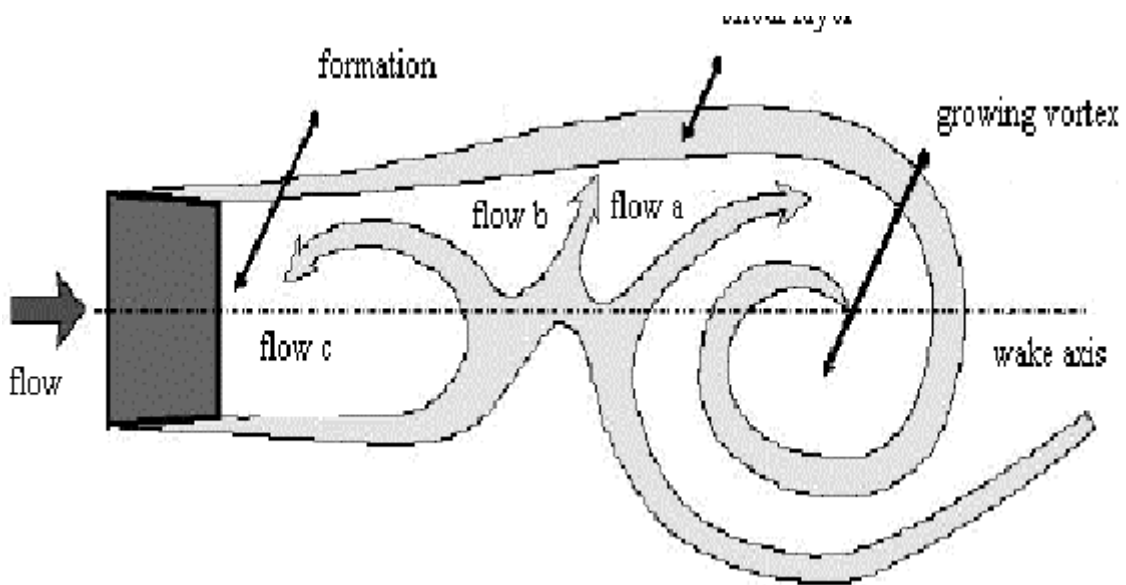


Figure 1.3 Vortex Interaction.

VORTICITY GENERATION; VORTEX STREET

Fluid particles come to rest at the surface of a stationary structure in a flow. This is the well-known no slip boundary condition which applies to all viscous fluid flows with the possible exception of certain hypersonic flows. The boundary layer is the thin layer of fluid adjacent to the surface of the structure through which the flow velocity increases from zero at the surface to the free stream velocity at the outer edge of the boundary layer. We may define a boundary layer Reynolds number based on span along the surface over which the boundary layer develops. There is a Reynolds number, on the order of 50, below which the wake, if it exists, is steady. Here we will be concerned with structures that generate thin, unsteady separated boundary layers in flows at Reynolds numbers above 50.

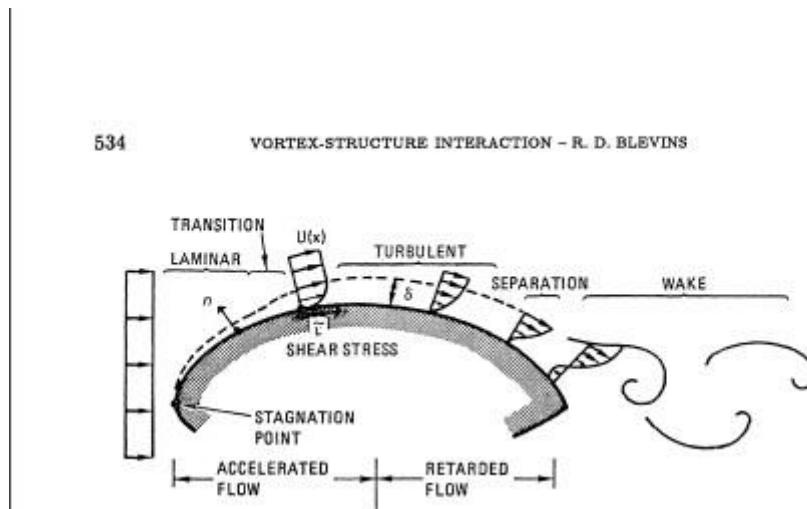


Figure 1.4 Vortex-Structure Interaction.

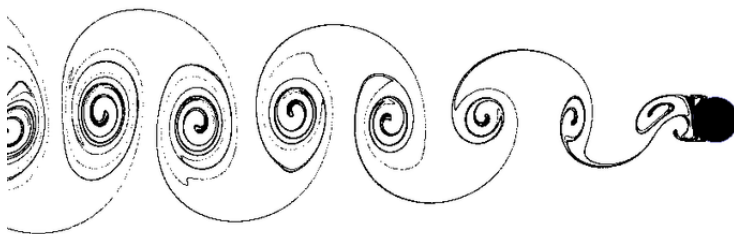


Figure 1.5 Von Karman Vortex Shedding.

VORTEX SHEDDING HAZARDS

Bridge oscillation: When wind flows over long structures like bridges, it can induce vortex shedding. These vortices can lead to dangerous oscillations in the bridge's structure. For instance, the Tacoma Narrows Bridge in the US collapsed in 1940 due to wind-induced vortex shedding.



Figure 1.6 Tacoma Narrow Bridge.

Lateral loads on tall buildings: Wind load is a crucial factor in designing tall buildings. Vortex shedding can cause lateral oscillations in buildings, leading to structural damage.

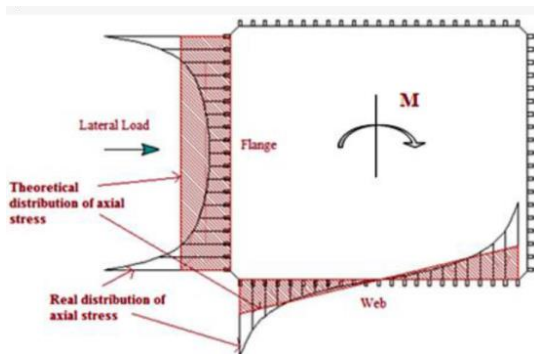


Figure 1.7 Lateral Load on Tall Buildings.

Transmission losses in power lines: Vortex shedding in high-voltage power lines can cause line oscillations, leading to transmission losses.

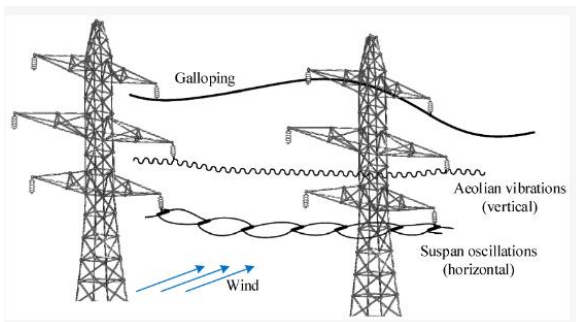


Figure 1.8 Oscillations on power lines.

WIND LOAD ANALYSIS

Wind load analysis, which involves the computation of forces exerted by the wind on structures, is a crucial aspect of structural engineering. Wind can exert significant lateral forces on a structure, which can cause it to sway or even collapse if it is not properly designed to withstand these loads.

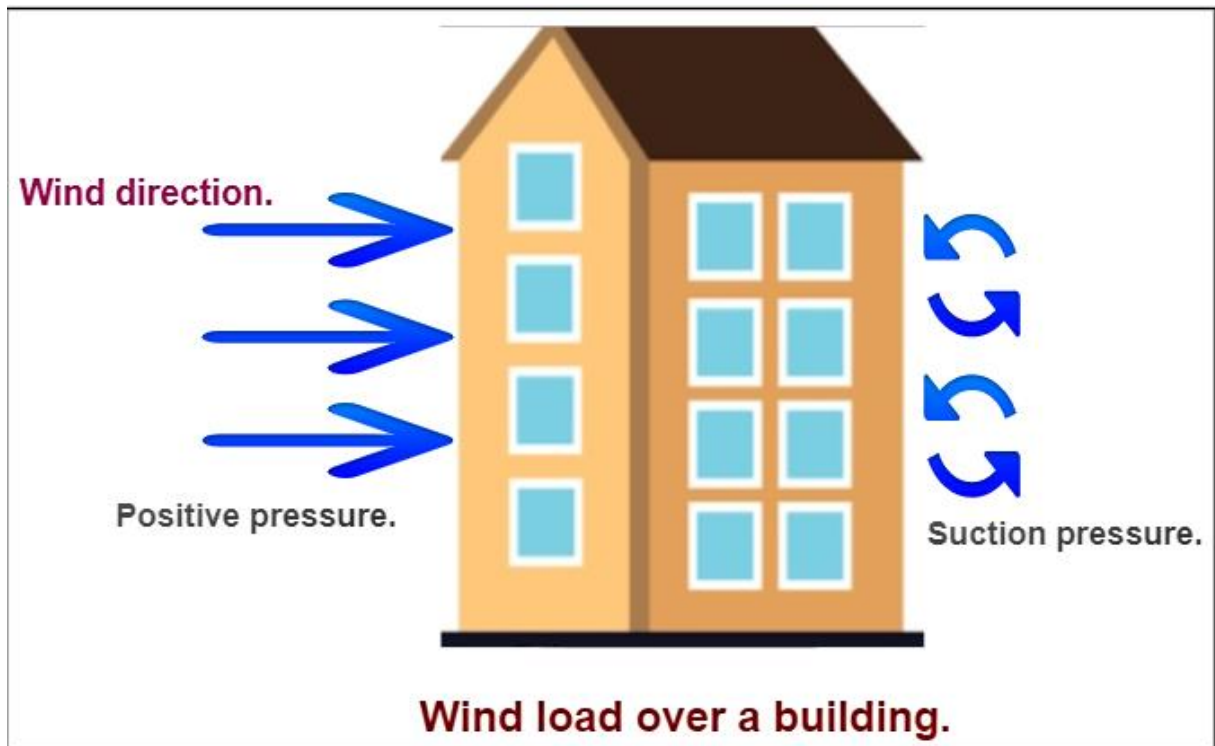


Figure 1.9 Wind Load Over A Building.

INTRODUCTION PING AN FINANCE CENTER

The Ping An Finance Center is a 115-storey, 599.1 m supertall skyscraper in Shenzhen, Guangdong, China. The building was commissioned by Ping An Insurance and designed by the American architectural firm Kohn Pedersen Fox Associates. The objective of this project is to oversee the wind load analysis and investigate vortex shedding phenomena on the Ping An Finance Center building.



Figure 2.0 Details of Building



Figure 2.1 Real Picture of the Building.

DETAILS AND DETERMINING SPECIFICATIONS OF PROPERTIES

The Ping An Finance Center is located in Shenzhen, China, where the average air temperature in Summer is approximately 29 degrees Celsius. Based on this information and the data provided in Figure 2.2, the dynamic viscosity and density of the air can be determined.

TABLE C.1 Physical Properties of Air at Standard Atmospheric Pressure (SI Units)^a

Temperature (°C)	Density, ρ (kg/m ³)	Dynamic viscosity, μ (N·s/m ²)	Kinematic viscosity, ν (m ² /s)	Specific heat ratio, γ
-40	1.514	1.57 E - 5	1.04 E - 5	1.401
-20	1.395	1.63 E - 5	1.17 E - 5	1.401
0	1.292	1.71 E - 5	1.32 E - 5	1.401
5	1.269	1.73 E - 5	1.36 E - 5	1.401
10	1.247	1.76 E - 5	1.41 E - 5	1.401
15	1.225	1.80 E - 5	1.47 E - 5	1.401
20	1.204	1.82 E - 5	1.51 E - 5	1.401
25	1.184	1.85 E - 5	1.56 E - 5	1.401
30	1.165	1.86 E - 5	1.60 E - 5	1.400
40	1.127	1.87 E - 5	1.66 E - 5	1.400
50	1.109	1.95 E - 5	1.76 E - 5	1.400
60	1.060	1.97 E - 5	1.86 E - 5	1.399
70	1.029	2.03 E - 5	1.97 E - 5	1.399
80	0.9996	2.07 E - 5	2.07 E - 5	1.399
90	0.9721	2.14 E - 5	2.20 E - 5	1.398
100	0.9461	2.17 E - 5	2.29 E - 5	1.397
200	0.7461	2.53 E - 5	3.39 E - 5	1.390
300	0.6159	2.98 E - 5	4.84 E - 5	1.379
400	0.5243	3.32 E - 5	6.34 E - 5	1.368
500	0.4565	3.64 E - 5	7.97 E - 5	1.357
1000	0.2772	5.04 E - 5	1.82 E - 4	1.321

^a Based on data from R. D. Blevins, *Applied Fluid Dynamics Handbook*, Van Nostrand Reinhold Co., Inc., New York, 1984.

Figure 2.2 Physical Properties of Air.

As previously mentioned, the average air temperature is assumed to be 29 degrees Celsius. Based on the data presented in Figures 2.3 and 2.4, an average wind velocity of 3.8 m/s is adopted for this analysis.

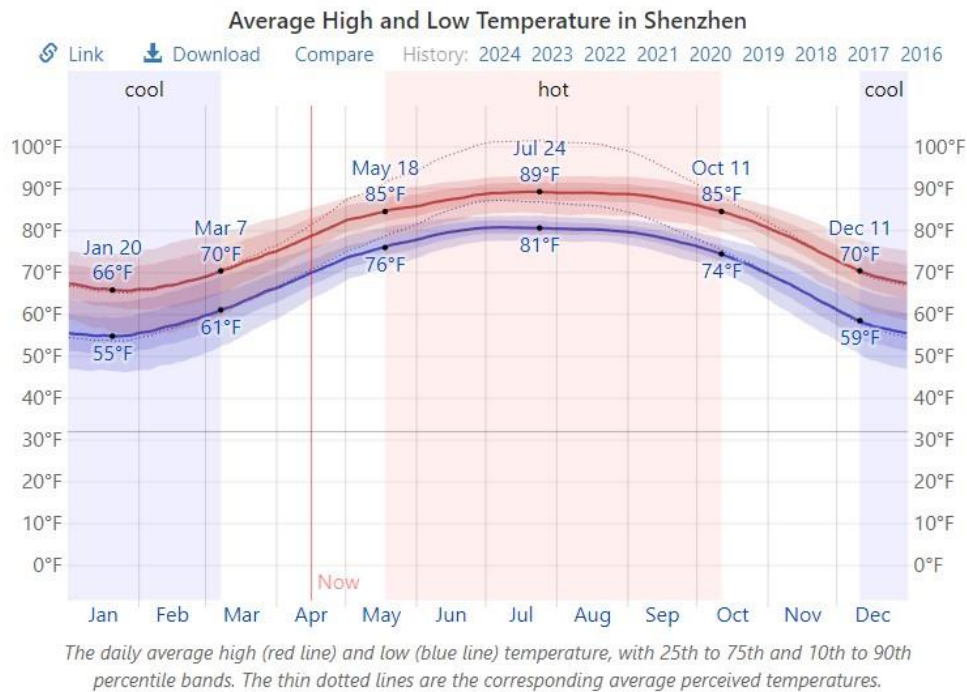


Figure 2.3 Average Temperature in Shenzhen.

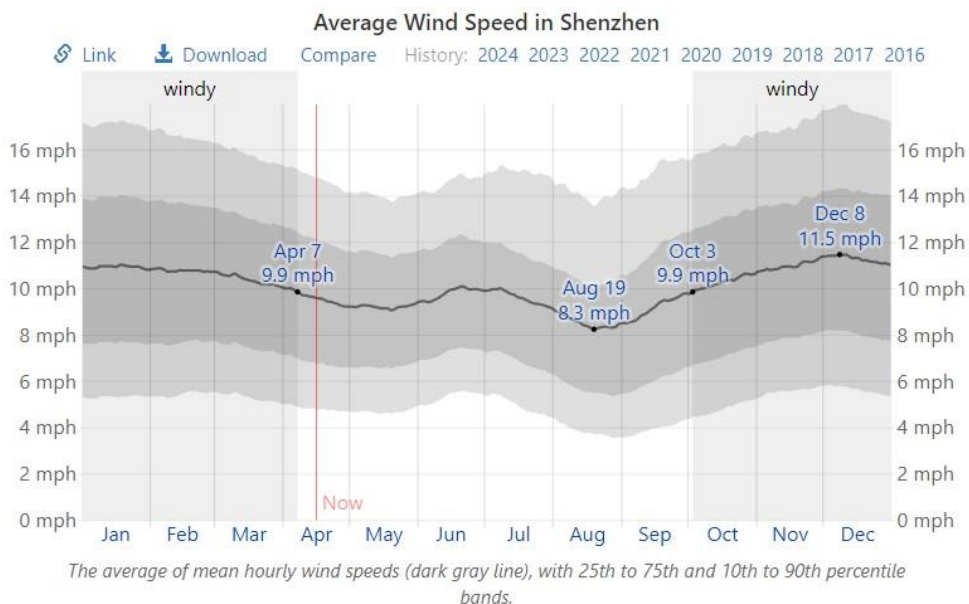


Figure 2.4 Average Wind Speed in Shenzhen.

CALCULATIONS OF IMPORTANT PARAMETERS OF THE ANALYSIS

Reynolds Number

Reynolds number (Re) is a dimensionless quantity that characterizes the flow regime around a bluff body, such as a cylinder. It represents the ratio of inertial forces to viscous forces acting on the fluid. Mathematically, it is expressed as:

$$Re = \frac{\rho v l}{\mu} = \frac{v l}{\nu}$$

v = Velocity of the fluid

l = The characteristics length, the chord width of an airfoil

ρ = The density of the fluid

μ = The dynamic viscosity of the fluid

ν = The kinematic viscosity of the fluid

Figure 2.6 Reynolds Number.

In this project;

Air density: $1.164 \frac{kg}{m^3}$

Velocity of Air: $15 \frac{m}{s}$

Characteristic Length: 50m

Dynamic Viscosity: $1.92 \times 10^{-5} \text{ kg } m^{-1} s^{-1}$

So Reynolds number;

$$Re = \frac{1.164 \times 15 \times 50}{1.92 \times 10^{-5}} = 45468750$$

According to figure 2.6 flow is fully turbulent.

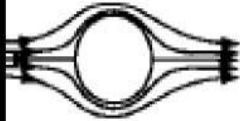




	No separation. Creeping flow	$Re < 5$
	A fixed pair of symmetric vortices	$5 < Re < 40$
	Laminar vortex street	$40 < Re < 200$
	Transition to turbulence in the wake	$200 < Re < 300$
	Wake completely turbulent. A: Laminar boundary layer separation	$300 < Re < 3 \times 10^5$ Subcritical

Figure 2.6 Critical Number for Reynolds in External Flows.

STROUHAL NUMBER

The Strouhal number (St) is a dimensionless parameter employed extensively in fluid dynamics and aerodynamics. It serves as a crucial indicator of oscillating flow phenomena, particularly in the context of vortex shedding.

$$St = \frac{f \cdot D}{V}$$

Where, St = Strouhal number

f = vortex shedding frequency

D = Diameter of the cylinder

V = Velocity of fluid

Figure 2.7 Strouhal Number.

Figure 2.8 illustrates that the Strouhal number obtained in this project is 0.3. Owing to the unique geometry of our system, a square geometry was adopted as the closest approximation to facilitate the application of the Strouhal number for analysis.

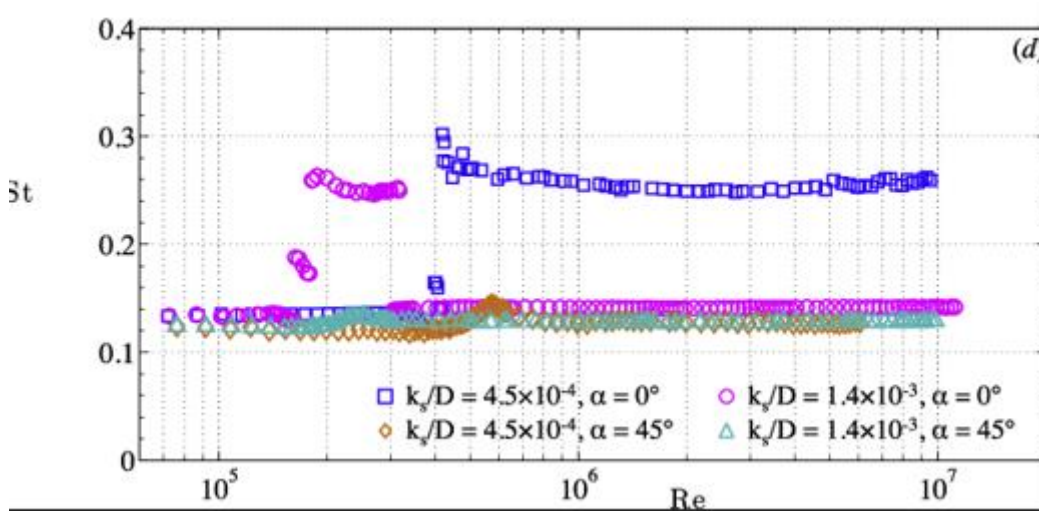


Figure 2.8 Strouhal Number for Different Geometries.

Strouhal number is ; 0.15

$$St = \frac{f x Lc}{v} = 0.15 = \frac{f x 50}{15} = 0.045$$

Frequency is : $0.045 \frac{1}{s}$

Period is : $\frac{1}{f} = 22.22$

TIME STEP SIZE

time step size (Δt) is a crucial parameter that dictates how the solution progresses through time. It represents the increment of time between each individual calculation within the simulation.

$$\Delta t = \frac{\Delta T}{20} = \frac{22.22}{20} = 0.875 \text{ s.}$$

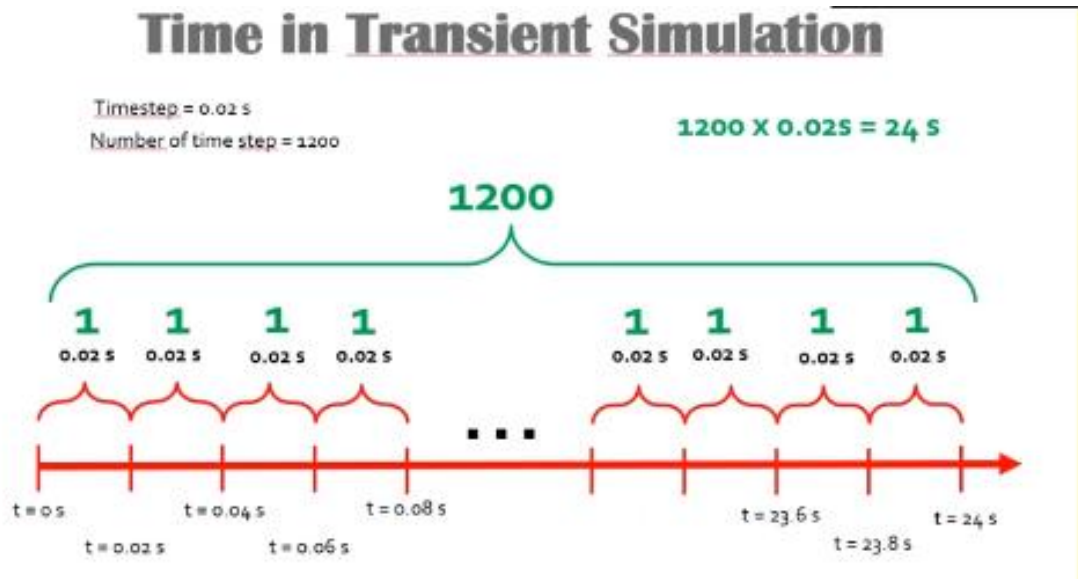


Figure 2.9 Time in Transient Simulation.

For a clearer comprehension of the parameters employed in the transient simulation, Figure 2.9 serves as a valuable resource.

This project aims to visualize the vortex shedding phenomenon within the solution animation, specifically targeting the depiction of six distinct vortex shedding events so ;

$$\text{Number of time step is ; } \frac{48 \times 22.22}{0.875} = 1200$$

ANALYSIS OF PING AN FINANCE CENTER IN ANSYS FLUENT

In the initial phase of our structural analysis, a two-dimensional geometrical representation will be employed. This simplified model will facilitate the visualization of vortex shedding phenomena within the subsequent solution animation.

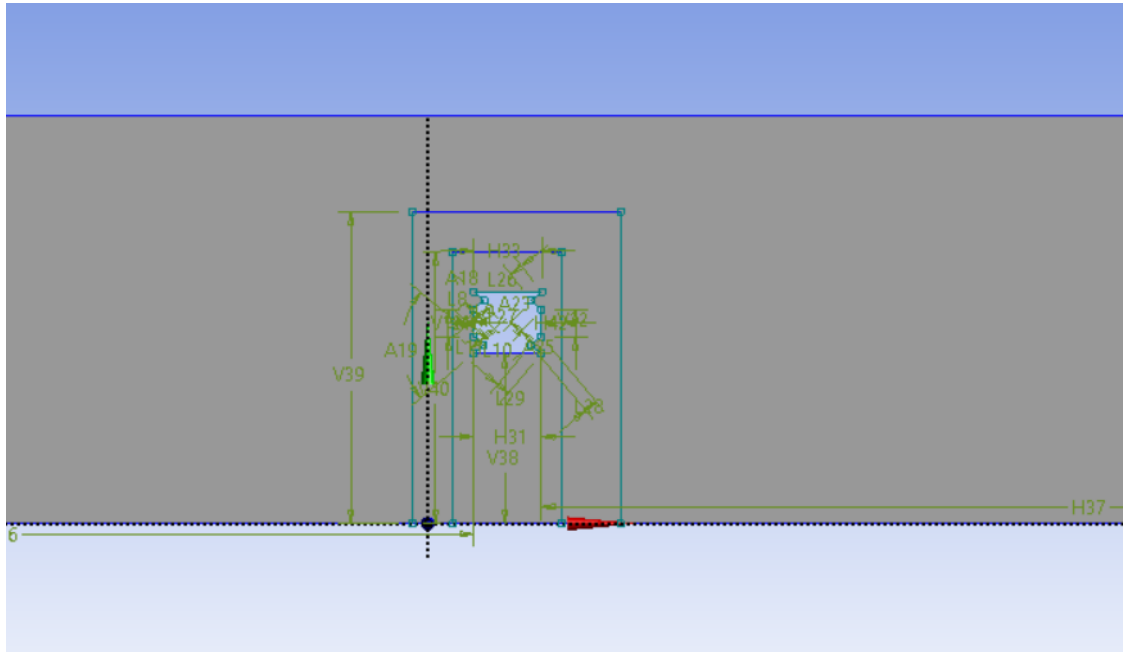


Figure 3.0 Geometry of Structure.

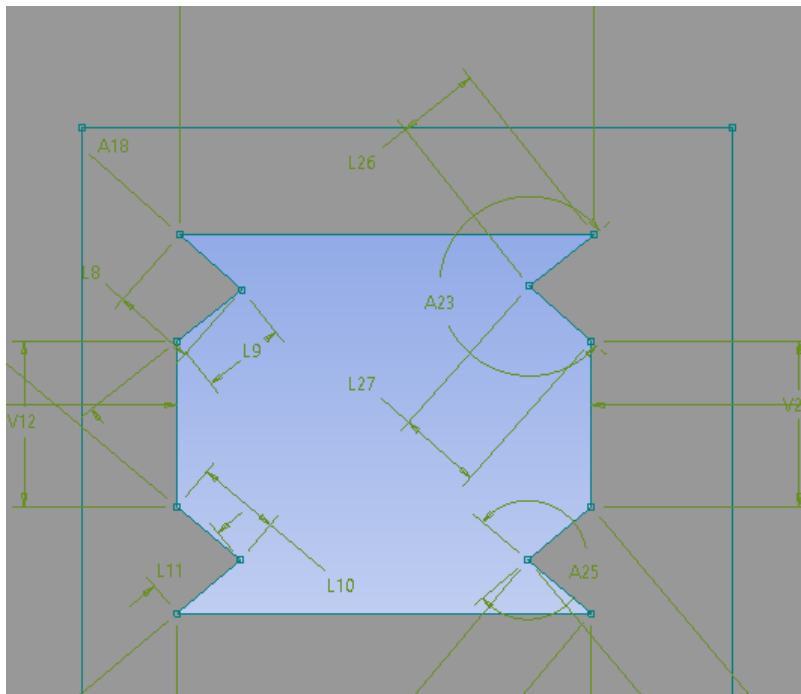


Figure 3.1 Closed View of Geometry.

Following the generation of the two-dimensional geometry, mesh generation presents a significant challenge due to the presence of critical points arising from the complex structural shape. Improper meshing can lead to floating-point errors in the solution, which occur when attempting to divide by zero – a mathematical impossibility. To address this critical step in the analysis and mitigate the risk of floating-point errors, a multizone quad/tri meshing method has been implemented.

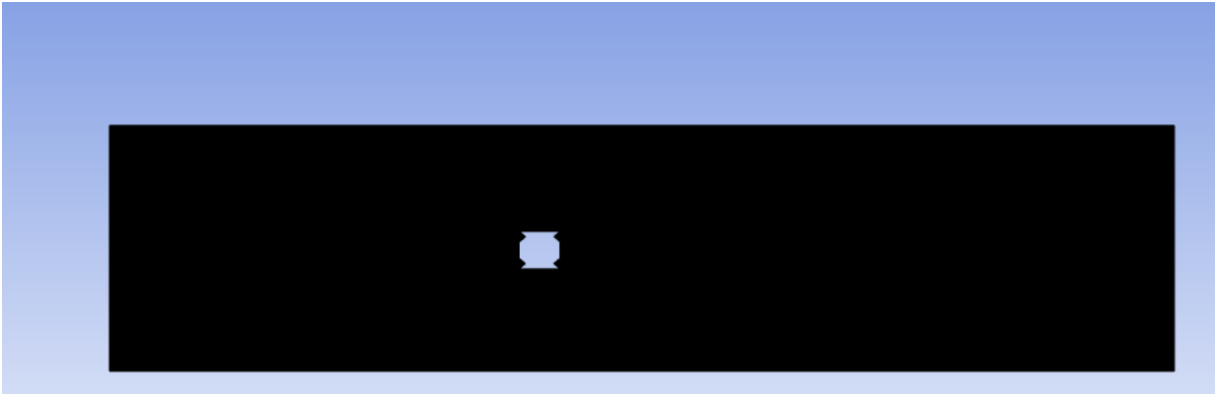


Figure 3.3 Meshed Structure.

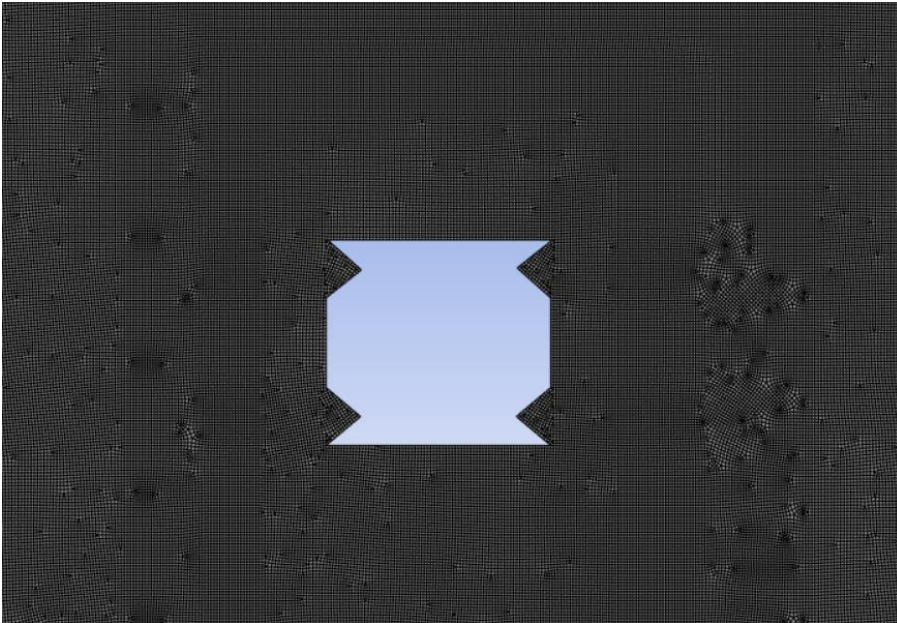


Figure 3.4 Meshed Stucture but Closer.

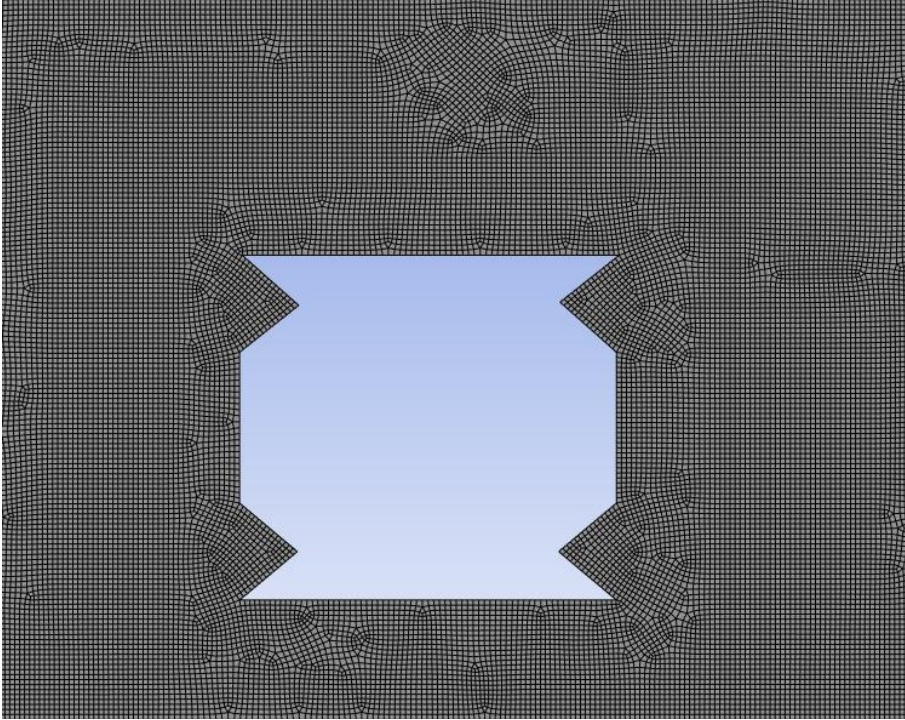


Figure 3.5 Closest Picture of Meshed Structure.

Beyond the selection of an appropriate meshing method, both the number of elements and their quality significantly impact the accuracy of the analysis. To achieve results closely approximating real-world behavior, a refined mesh with high-quality elements is essential. While orthogonal elements are generally preferred due to their superior accuracy, skewness is another crucial quality metric to be evaluated.

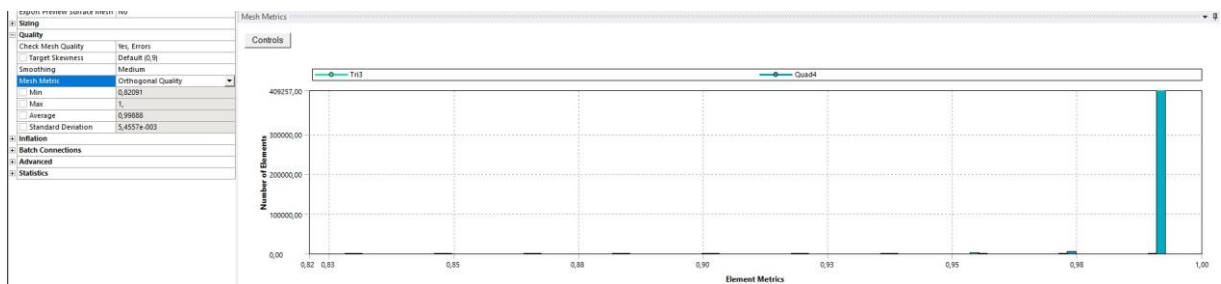


Figure 3.6 Mesh Quality for Orthogonal.

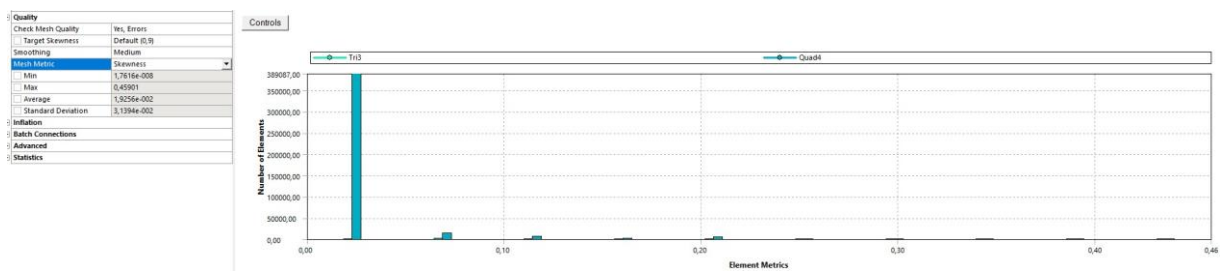


Figure 3.7 Mesh Quality for Skewness.

Statistics	
<input type="checkbox"/> Nodes	417971
<input type="checkbox"/> Elements	417414
Show Detailed Statistics	No

Figure 3.8 Number of Mesh.



Figure 3.9 Skewness and Orthogonal Mesh Metric Spectrums.

Following mesh generation, the final step involves defining the simulation parameters within ANSYS Fluent. Prior to initiating the solution process, a thorough quality check of these settings is crucial. Omitting this step can lead to errors during the solution phase, potentially resulting in significant time expenditure due to the computationally intensive nature of the analysis, particularly when employing standard computing resources.

Following mesh generation and quality evaluation, the gravitational acceleration was defined within the ANSYS Fluent setup. A pressure-based solver was chosen due to its suitability for incompressible flows, which characterizes this analysis. While the flow velocity is relatively low, the computational efficiency offered by the pressure-based approach outweighs potential benefits of a density-based solver in this specific case. Considering the two-dimensional, planar nature of the analysis and the inherent complexity of the flow (which might preclude convergence in a steady-state simulation), a transient solution approach was deemed necessary. In selecting an appropriate turbulence model for this analysis, the k-omega SST model has been prioritized. This choice is grounded in its well-established reputation as the industry standard within computational fluid dynamics (CFD) applications. Notably, the k-omega SST model demonstrates superior capabilities in predicting flow separation compared to many other

Reynolds-Averaged Navier-Stokes (RANS) models. Furthermore, it exhibits favorable behavior in adverse pressure gradients, a characteristic potentially relevant to the current analysis.

Leveraging our prior knowledge of the fluid's properties, specifically density and viscosity, and considering the air as the working fluid in this analysis, the appropriate material properties were input into the program.

Based on our previous discussions, the inlet air velocity has been defined as 3.8 m/s. Since we are simulating atmospheric conditions, no initial gauge pressure is specified. To account for turbulence in this external flow, the standard $k-\varepsilon$ model (or another appropriate model) will be employed along with a turbulence intensity of 5% and a turbulent viscosity ratio of 10. The selection of these specific values for the external flow is considered appropriate for this analysis. For the outlet boundary conditions in this analysis, the default settings will be retained. Dynamic mesh is frequently utilized in simulations of rotating equipment, oscillating structures, or fluid-structure interactions. Additionally, it is employed in simulations of free-surface flows in which the fluid domain's form changes over time.

The selection of appropriate reference values is crucial for this analysis, particularly when evaluating key parameters such as lift, drag, and surface area. Accurate reference values ensure a meaningful interpretation of these force and geometric quantities.

Due to its inherent advantages, the Pressure-Implicit with Splitting Operators (PISO) scheme emerges as a valuable tool for specific transient simulations within ANSYS Fluent, particularly those involving incompressible flows. PISO offers several benefits compared to simpler pressure-velocity coupling schemes like SIMPLE. Firstly, it achieves stable solutions in fewer iterations per time step, leading to reduced computational times for transient analyses.

Secondly, PISO employs additional pressure corrections within each time step, enhancing the accuracy of the pressure-velocity coupling. This improved accuracy is crucial for capturing the time-dependent behavior accurately in transient simulations. Finally, PISO demonstrates superior robustness when dealing with complex flows or poorly conditioned meshes, a characteristic that proves beneficial for transient simulations involving unsteady flow phenomena.

In ANSYS Fluent, the convergence criteria are typically set to an absolute value of 1×10^{-3} . However, due to the critical nature of the results in this specific analysis, a stricter convergence criterion of 1×10^{-6} was employed. This more stringent setting enhances the accuracy of the simulation by requiring a greater reduction in the residuals between subsequent iterations.

For transient simulations, it has been established that employing a hybrid initialization approach may not yield the most accurate results. Consequently, a standard initialization strategy, followed by computation from the inlet boundary ("in"), has been identified as the optimal approach for this specific analysis.

Finally, the timestep size and total number of timesteps, previously determined through careful calculations, are entered into the ANSYS Fluent setup. With these parameters defined, the computational analysis can be initiated.

DISCUSSING THE RESULT OF ANALYSIS

For transient simulations, achieving convergence of scaled residuals is a critical first step in assessing the validity of the solution. In this analysis, the convergence criterion for scaled residuals was satisfied at the end of each iteration, indicating a successful simulation from a convergence standpoint.

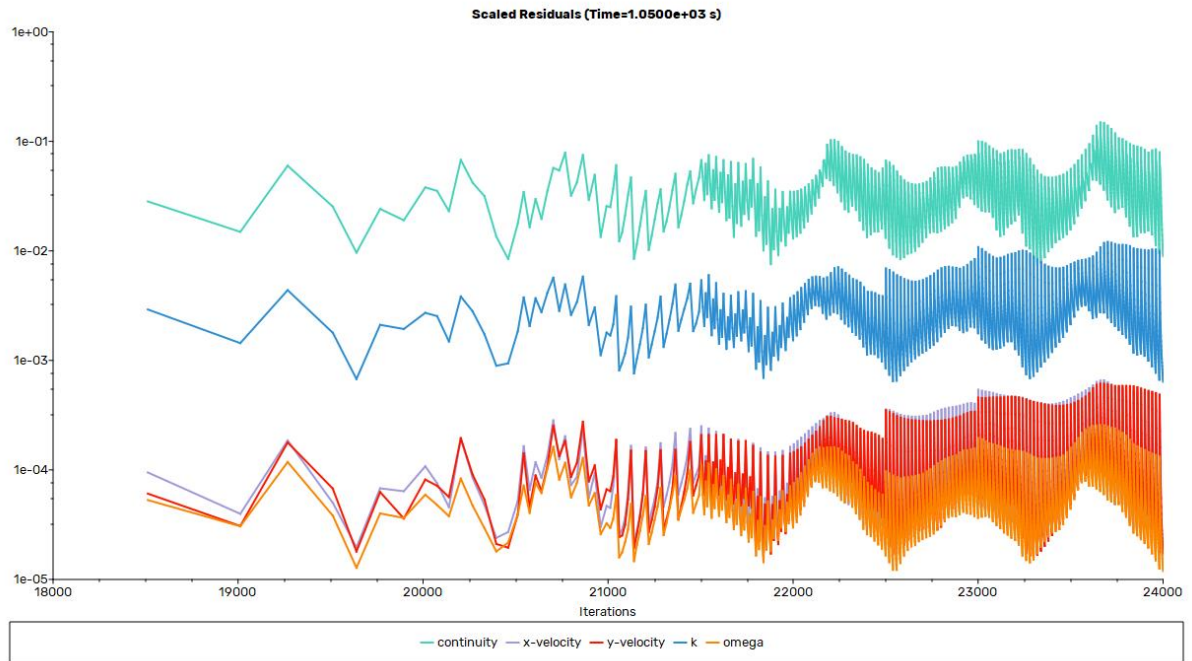


Figure 4.0 Scaled Residuals.

Our analysis yielded a drag coefficient of approximately 2.4, which aligns with the value depicted for a square in Figure 4.1. However, it is important to acknowledge that the analyzed object deviates slightly from a perfect square, resembling more closely the second shape presented in Figure 4.2, where the drag coefficient is observed to be 2.2.

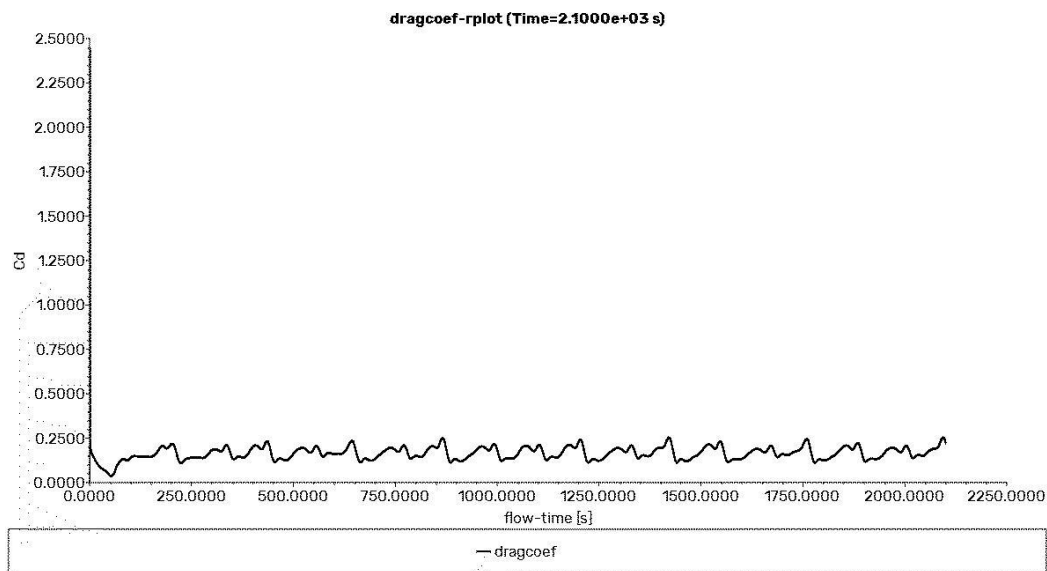


Figure 4.1 Drag Coefficient Graph.


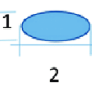
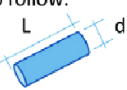
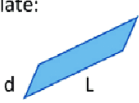
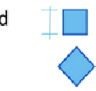
Body (Flow From left to right)	L/d	Re= $V d/\nu$	C_D
Bodies of revolution			
1) Sphere: 		10^5 $>3 \times 10^5$	0.50 0.20
2) Ellipsoid: d=1 		$>2 \times 10^5$	0.07
3) Circular cylinder axis vertical to flow: 	1 5 20 ∞ 5 ∞	10^5 $>5 \times 10^5$	0.63 0.74 0.90 1.20 0.35 0.33
4) Rectangular plate: L=length d= width 	1 5 20 ∞	$>10^3$	1.16 1.20 1.50 1.90
5) Square cylinder: 		3.5×10^4 $10^4 - 10^5$	2.0 1.6

Figure 4.2 Cd Values For Different Shapes.

While comprehensive online resources on the impact of geometry on lift forces can be limited, the results obtained through my Fast Fourier Transform (FFT) analysis suggest that the lift generated in this case appears to be within acceptable parameters.

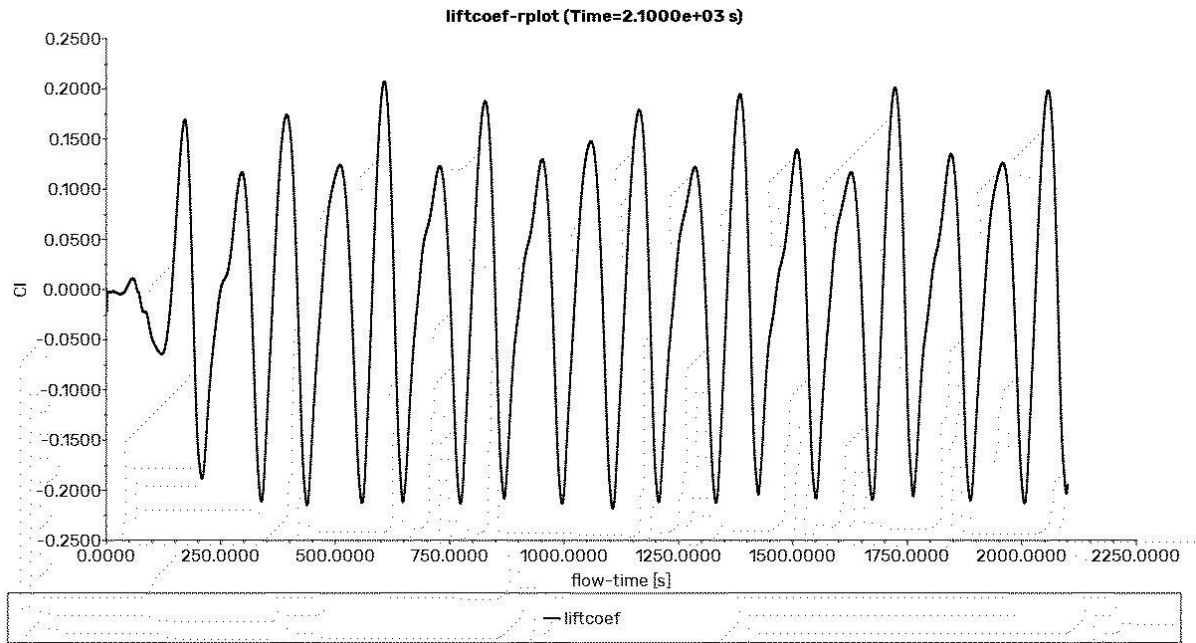


Figure 4.3 Lift Coefficient Graph.

Our Fast Fourier Transform (FFT) analysis yielded a dominant frequency of approximately 0.04, from the previously calculated value of 0.045. This discrepancy could be attributed to the non-square geometry of the analyzed structure. While square geometries are often used for theoretical calculations due to their simplicity, real-world objects may deviate from this ideal shape.

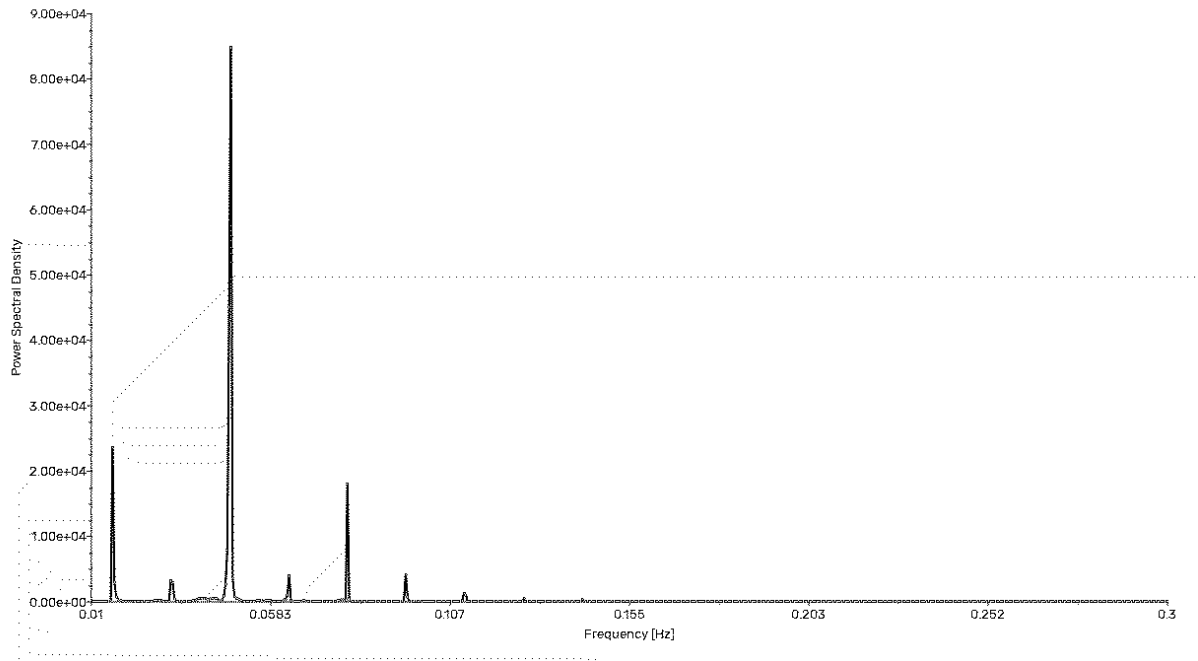


Figure 4.4 FFT Graph.

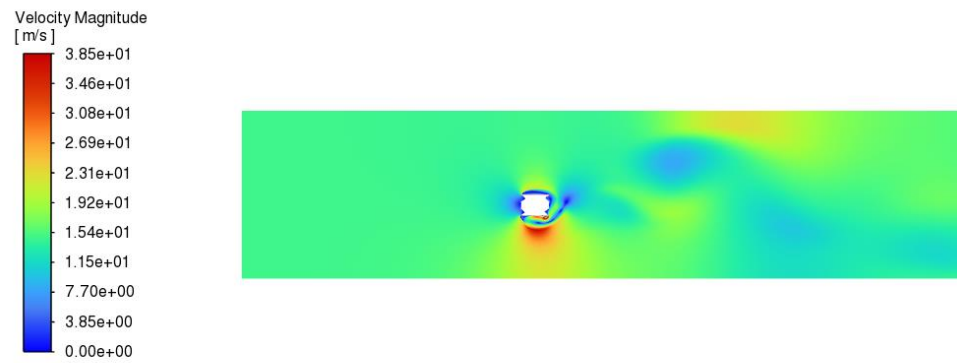


Figure 4.5 Velocity Contour.

OTHER ANALYSES RESULTS

The figures of 4.0-4.5 pertain to a velocity of 15 m/s. However, this velocity is too low for relevant skyscraper applications. Therefore, further analyses will be conducted at velocities of 20 m/s, and 25 m/s. It is important to note that for all these velocities, the Mach number remains below 0.3. Consequently, we can assume incompressible air flow throughout the analyses.

FFT GRAPH FOR DIFFERENT ANALYSES

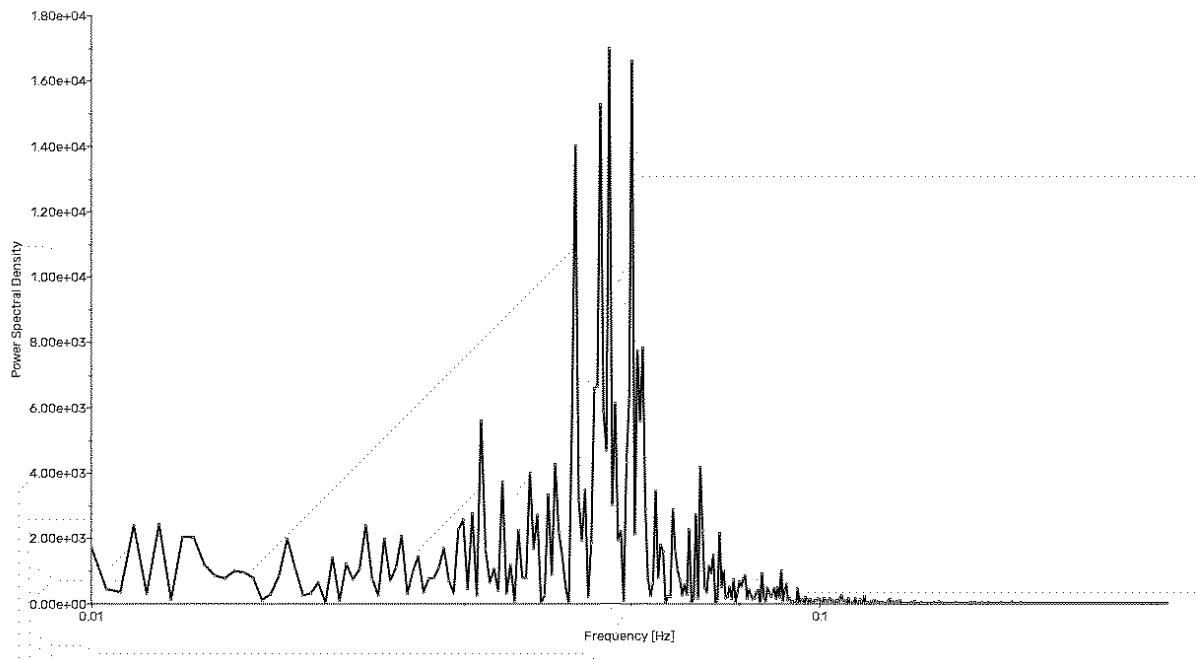


Figure 4.6 FFT Graph of 20m/s.

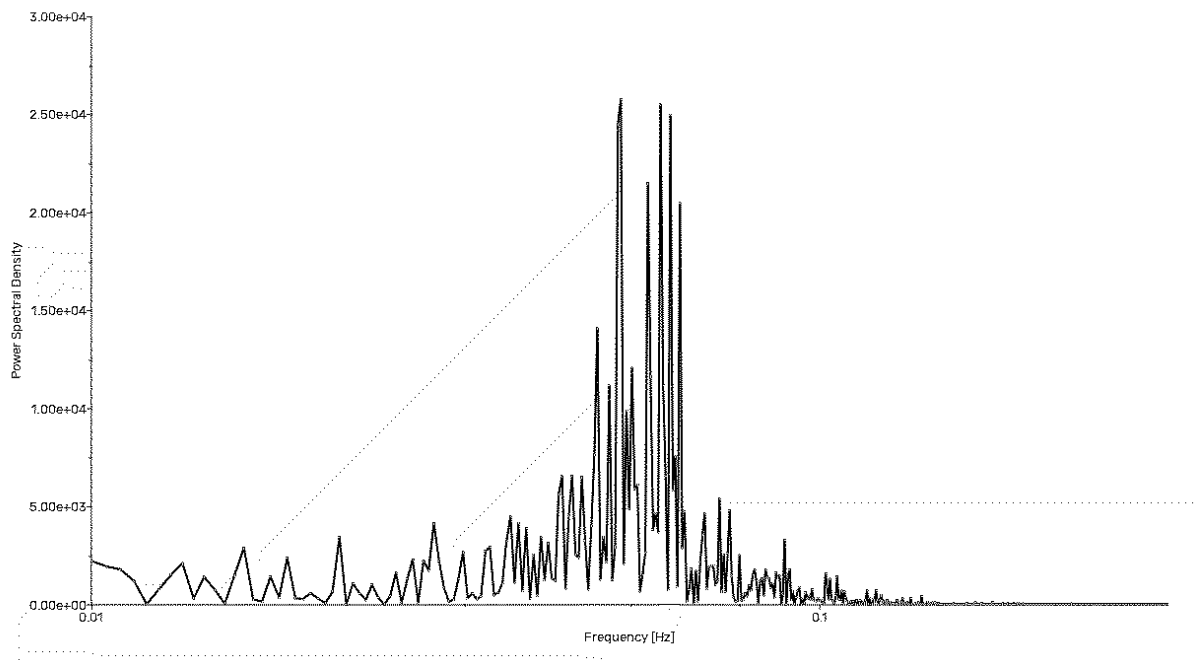


Figure 4.7 FFT Graph of 25m/s.

VELOCITY CONTOURS OF ANALYSES

Ansys
2024 R1
STUDENT

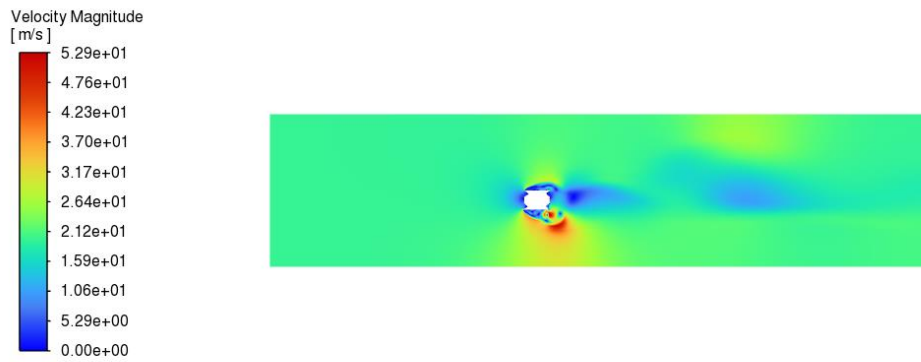


Figure 4.8 Velocity Contour of 20m/s.

Ansys
2024 R1
STUDENT

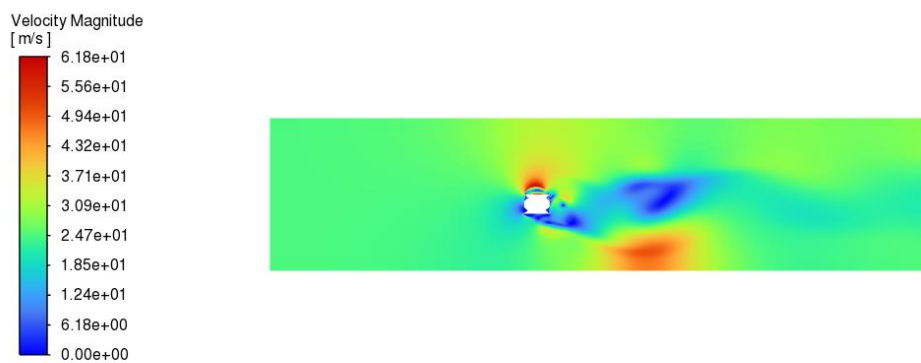


Figure 4.9 Velocity Contour of 25m/s.

RESULT OF ANALYSIS

Initially, the obtained frequency may appear very low. However, further research indicates that vortex shedding frequencies for skyscrapers typically fall within this range, validating our analysis. Our calculations place the vortex shedding frequency between 0.045 Hz and 0.06 Hz. Critically, the building's natural frequency should not lie within this range to avoid resonance.



Figure 4.10 Ping An Finance Center.

REFERENCES

- Asghari Mooneghi, M. and Kargarmoakhar, R. 2016 Aerodynamic Mitigation and Shape Optimization of Buildings: Review. *Journal of Building Engineering* 6:225-235
- Cochran 2012 Wind Issues in the Design of Buildings. In *Wind Issues in the Design of Buildings* pp. 1-16.
- Li Y., Tian X., Tee K. F., Li Q. and Li Y. 2018 Aerodynamic treatments for reduction of windloads on high-rise buildings *Journal of Wind Engineering and Industrial Aerodynamics* 172:107-115
- Xie, J. 2014 Aerodynamic optimization of super-tall buildings and its effectiveness assessment *Journal of Wind Engineering and Industrial Aerodynamics* 130: 88-98.
- Xie, J. and Yang, X. 2019 Exploratory study on wind-adaptable design for super-tall buildings *Wind and Structures* 29: 489-497.
- Tschanz T. and Davenport A. G. 1983 The base balance technique for the determination of dynamic wind loads. *Journal of Wind Engineering and Industrial Aerodynamics* 13: 429-439
- Barriga, A.R., Crowe, C.T. and Robertson, J.A., 1975, "Pressure Distribution of a Square Cylinder at a Small Angle of Attack in a Turbulent Cross Flow", *Proceedings of the Fourth International Conference on Wind Effects on Buildings and Structures*, London, United Kingdom, pp. 89-93.
- Lee, B.E., 1975, "The Effect of Turbulence on the Surface Pressure Field of a Square Prism", *Journal of Fluid Mechanics*, Vol. 69, Part 2, pp. 263-282.
- Mandal, A.C. and Farok, G.M.G., 2005 "An Experimental Investigation of Static Pressure Distributions on Square and Rectangular Cylinders with Rounded Corners", 4th International Conference on Heat Transfer, Fluid Mechanics and Thermodynamics (HEFAT 2005), Cairo, Egypt, Paper No. MA5.
- T. Tamura, T. Miyagi, "The Effect of Turbulence on aerodynamic forces on a square cylinder with various corner shapes", *The Fourth Asia-Pacific Symposium on Wind Engineering*, 14-16 July, 1997, Australia
- Rimas Vaicaitis "Response Analysis of Tall Buildings To Wind Loadings"
https://www.researchgate.net/publication/285661860_Response_Analysis_of_Tall_Buildings_to_Wind_Loadings.